PERGAMON

International Journal of Solids and Structures 39 (2002) 5945–5962

INTERNATIONAL JOURNAL OF SOLIDS and STRUCTURES

www.elsevier.com/locate/ijsolstr

Dynamic analysis of laminated cross-ply composite non-circular thick cylindrical shells using higher-order theory

M. Ganapathi *, B.P. Patel, D.S. Pawargi

Institute of Armament Technology, Girinagar, Pune 411 025, India

Received 28 January 2002; received in revised form 16 August 2002

Abstract

Here, the dynamic analysis of laminated cross-ply composite non-circular thick cylindrical shells subjected to thermal/mechanical load is carried out based on higher-order theory. The formulation accounts for the variation of the in-plane and transverse displacements through the thickness, abrupt discontinuity in slope of the in-plane displacements at the interfaces, and includes in-plane, rotary inertia terms, and also the inertia contributions due to the coupling between the different order displacement terms. The strain–displacement relations are accurately accounted for in the formulation. The shell responses are obtained employing finite element approach in conjunction with direct time integration technique. A detailed parametric study is carried out to bring out the effects of length and thickness ratios, eccentricity parameters and number of layers on the thermal/mechanical response characteristics of non-circular shells.

Keywords: Laminated shell; Cross-ply; Response; Non-circular; Higher order; Finite element

1. Introduction

In many engineering applications, the cylinders are used as primary structural members because of their high structural efficiency. Due to the advent of composite materials, composite cylinders are of particular interest in the design of lightweight and efficient structures, especially in the aerospace industry. While circular cylinders are perhaps the most common, due to the design considerations, for instance in submersibles, flight structures etc., cylindrical shells with non-circular cross-sections are preferred. Most of these structures are, in general, subjected to thermal/mechanical loads and dynamic environment during their operation. Hence, the study of dynamic behavior of such non-circular cylindrical shell structures through accurate modeling is important in assessing the failure and has recently attracted the attention of researchers.

The vibration analysis of circular cylindrical shells has received considerable attention in the literature and has been reviewed by Leissa (1973), and, more recently, by Noor (1990), Noor and Burton (1990),

* Corresponding author. Tel.: +91-20-4389550; fax: +91-20-4389509.
E-mail address: mganapathi@hotmail.com (M. Ganapathi).

0020-7683/02/$ - see front matter
PII: S0020-7683(02)00495-X

Qatu (1992) and Soldatos (1994). However, the number of studies that deal with the behavior of non-circular cylinders is rather limited and reviewed by Soldatos (1999). This is possibly due to the difficulty introduced in governing equations because of the cross-sectional radius of curvature as a function of an arc co-ordinate. It may be concluded from the literature that few contributions are available concerning with free vibration analysis of anisotropic laminated non-circular cylindrical shells compared to those of isotropic case, and they are cited here. The free vibration of laminated non-circular case has been analyzed employing classical theory (Soldatos and Tzivanidis, 1982; Soldatos, 1984; Hui and Du, 1986; Suzuki et al., 1994), and using first-order shear deformation theory (Noor, 1973; Kumar and Singh, 1995; Suzuki et al., 1996). The theory assuming parabolic variation of thickness shear for the study of composite non-circular shells has been attempted (Soldatos, 1987; Kumar and Singh, 1996). The Galerkin procedure was employed in the work of Soldatos and Tzivanidis (1982), Soldatos (1984), Soldatos (1987) and Hui and Du (1986) whereas the power series expansion method was adopted in the work of Suzuki et al. (1994, 1996). Noor (1973) solved the problem using multilocal difference discretization method while the energy approach was applied by Kumar and Singh (1995, 1996). In all these investigations, the analysis has been carried out using analytical approaches, and has been limited to free vibrations of cross-ply non-circular shells. To the best of authors' knowledge, there is no study available in the literature pertaining to the dynamic response of non-circular composite cylindrical shells, and even isotropic case has not received adequate consideration, except the work of Cheung et al. (1991) that concerns with thin isotropic shell based on classical theory.

It can be opined from the existing literature that, in general, the first-order theory that requires an arbitrary shear correction to the transverse shear stiffness is fairly accurate for the estimation of global behaviors like deflections, fundamental frequency and buckling load of moderately thick composite laminates. However, it is inadequate for the estimation of higher-order frequencies, mode shapes, large deflections and distribution of stresses. This has necessitated the introduction of higher-order function in the displacement model, and layer-wise theory for the study of circular cylindrical shells (Bhimaraddi, 1984; Bhaskar and Vardan, 1991; Di Sciuva and Icardi, 1993; He, 1994; Icardi, 1998; Ganapathi et al., 2002). To the authors' knowledge, the application of such models involving higher-order expansions of the displacement fields in powers of the thickness co-ordinate yielding both the transverse shear and the transverse normal deformation is not commonly available yet in the literature for the analysis of laminated non-circular cylindrical cases. Furthermore, the studies employing the improved approximate technique such as finite element method, which can easily handle a more general case of loading, complicated boundary conditions and complexity due to the advanced composite materials, for the non-circular cylindrical case seems to be scarce in the literature.

Here, a higher-order theory with through the thickness approximation of in-plane and transverse displacements for the laminates (Makhecha et al., 2001a; Ganapathi et al., 2002) is extended to analyze the transient response characteristics of laminated cross-ply non-circular cylindrical shells subjected to thermal/mechanical loads based on finite element procedure. The formulation is, general, in the sense that it is applicable for arbitrary variation in the cross-section of the cylindrical shells. The element used is a C^0 eight-noded field consistent shell element with 13 degrees of freedom per node. The strain–displacement relationship is accurately introduced in the formulation. All the inertia terms, due to the parts resulting from first-order model, the higher-order displacement function, and the coupling between the different order displacements are included in evaluating the kinetic energy. The structural responses are evaluated using Newmark integration scheme. The accuracy of the present model is checked against the available analytical/three-dimensional solutions. A detailed parametric study is carried out to bring out the effects of variations of non-circularity, thickness and length ratios, and number of layers on the dynamic characteristics of non-circular cross-ply cylindrical shells with elliptical cross-section. The results evaluated here demonstrate the profound importance of the inclusion of through-thickness variation and slope discontinuity in the displacement kinematics on the response of non-circular shells.

2. Formulation

A laminated composite non-circular cylindrical shell is considered with the co-ordinates x along the meridional direction, y along the circumferential direction and z along the thickness direction having origin at the middle-surface of the shell as shown in Fig. 1. Based on Taylor's series expansion method for deducing the two-dimensional formulation of a three-dimensional elasticity problem, the in-plane displacements u^k and v^k, and the transverse displacement w^k for the kth layer, are assumed as

$$\begin{aligned} u^k(x,y,z,t) &= u_0(x,y,t) + z\theta_x(x,y,t) + z^2\beta_x(x,y,t) + z^3\phi_x(x,y,t) + S^k\psi_x(x,y,t) \\ v^k(x,y,z,t) &= v_0(x,y,t) + z\theta_y(x,y,t) + z^2\beta_y(x,y,t) + z^3\phi_y(x,y,t) + S^k\psi_y(x,y,t) \\ w^k(x,y,z,t) &= w_0(x,y,t) + zw_1(x,y,t) + z^2\Gamma(x,y,t) \end{aligned} \tag{1}$$

Here, u_0, v_0, w_0 are the displacements of a generic point on the reference surface; θ_x, θ_y are the rotations of normal to the reference surface about the y and x axes, respectively; w_1, β_x, β_y, Γ, ϕ_x, ϕ_y are the higher-order terms in the Taylor's series expansions, defined at the reference surface. ψ_x and ψ_y are generalized variables associated with the zigzag function, S^k.

The zigzag function, S^k, as given in the work of Murukami (1986), is defined by

$$S^k = 2(-1)^k z_k/h_k \tag{2}$$

where z_k is the local transverse co-ordinate with its origin at the centre of the kth layer and h_k is the corresponding layer thickness. Thus, the zigzag function is piecewise linear with values of -1 and 1 alternately at the different interfaces. The 'zigzag' function, as defined above, takes care of the inclusion of the slope discontinuity of u and v at the interfaces of the laminate as observed in exact three-dimensional elasticity solutions of thick laminated composite structures. The use of such function is more economical than a

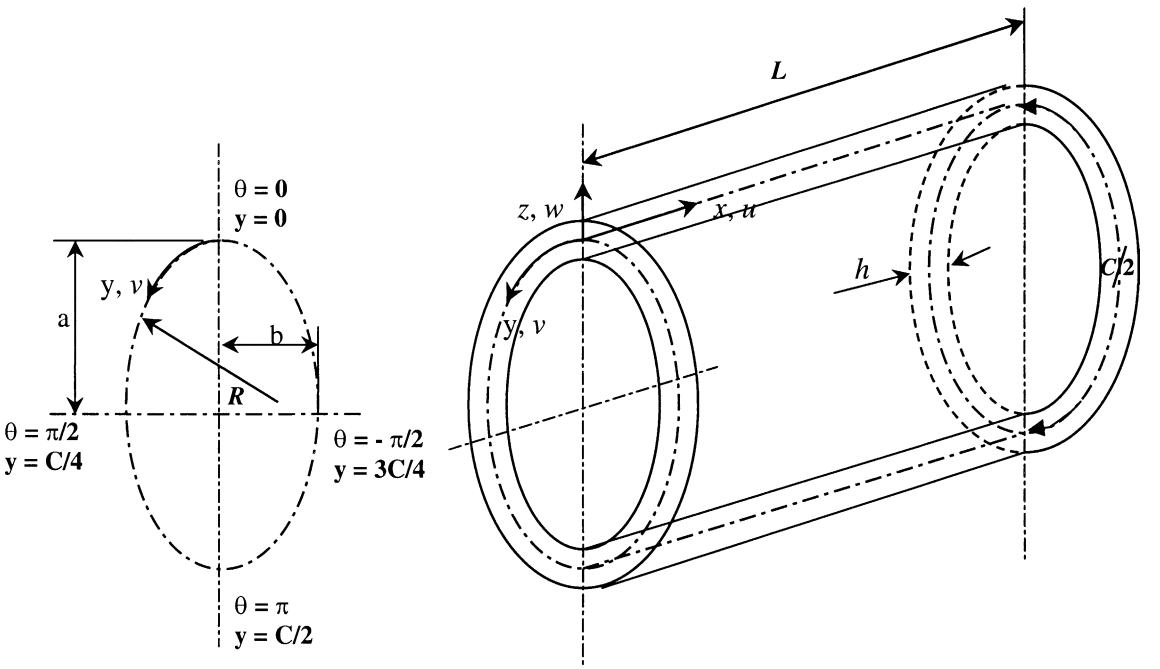

Fig. 1. Generalized co-ordinate system and cross-sectional details of the elliptical shell.

discrete layer approach of approximating the displacement variations over the thickness of each layer separately. Although both these approaches account for slope discontinuity at the interfaces, in the discrete layer approach the number of unknowns increases with the increase in the number of layers, whereas it remains constant in the present approach.

The strains in terms of middle-surface deformation, rotations of normal, and higher-order terms associated with displacements for kth layer are as,

$$\{\varepsilon\} = \left\{ \begin{array}{c} \varepsilon_{\mathrm{bm}} \\ \varepsilon_{\mathrm{s}} \end{array} \right\} - \left\{ \begin{array}{c} \bar{\varepsilon}_{\mathrm{t}} \\ 0 \end{array} \right\} \tag{3}$$

The vector $\{\varepsilon_{\mathrm{bm}}\}$ includes the bending and membrane terms of the strain components and vector $\{\varepsilon_{\mathrm{s}}\}$ contains the transverse shear strain terms. These strain vectors are accurately introduced in the formulation and are defined as (Kraus, 1967; Bhaskar and Vardan, 1991; Rao and Ganesan, 1996; Qatu, 1999)

$$\left\{ \begin{array}{c} \varepsilon_{\mathrm{bm}} \\ \varepsilon_{\mathrm{s}} \end{array} \right\} = \left\{ \begin{array}{c} \varepsilon_{xx} \\ \varepsilon_{yy} \\ \varepsilon_{zz} \\ \gamma_{xy} \\ \gamma_{xz} \\ \gamma_{yz} \end{array} \right\} = \left\{ \begin{array}{c} u^k_{,x} \\ (v^k_{,y} + w^k/R)/(1 + z/R) \\ w^k_{,z} \\ u^k_{,y}/(1 + z/R) + v^k_{,x} \\ u^k_{,z} + w^k_{,x} \\ v^k_{,z} + (w^k_{,y} - v^k/R)/(1 + z/R) \end{array} \right\} \tag{4a}$$

where the subscript comma denotes the partial derivative with respect to the spatial co-ordinate succeeding it. R, the principal radii of curvature in the circumferential direction, is function of circumferential co-ordinate y. The variation of R in the circumferential direction depends on the type of cross-section i.e. for instance, for elliptical cross-section, R can be described as (Suzuki et al., 1996)

$$R = (b^2/R_0)(1 + \mu_0 \cos 2\theta)^{-3/2} \tag{4b}$$

where $R_0 (= [(a^2 + b^2)/2]^{1/2})$ is the representative radius, $\mu_0 = (a^2 - b^2)/(a^2 + b^2)$; and θ is a variable that denotes an angle between the tangent at the origin of y (circumferential co-ordinate) and the one at any point on the middle-surface. a, b are the lengths of semi-major and semi-minor axes of elliptical cross-section.

Using the kinematics given in Eq. (1), Eq. (4a) can be rewritten as

$$\left\{ \begin{array}{c} \varepsilon_{\mathrm{bm}} \\ \varepsilon_{\mathrm{s}} \end{array} \right\} = [\bar{Z}]\{\bar{\varepsilon}\} \tag{5a}$$

where

$$[\bar{Z}] = \begin{bmatrix} Z_1 & Z_2 & Z_3 & Z_4 & Z_5 & O_1 & O_1 & O_1 & O_1 & O_2 \\ O_1^{\mathrm{T}} & O_1^{\mathrm{T}} & O_1^{\mathrm{T}} & O_1^{\mathrm{T}} & O_2^{\mathrm{T}} & Z_6 & Z_7 & Z_8 & Z_9 & Z_{10} \end{bmatrix} \tag{5b}$$

$$\{\bar{\varepsilon}\} = \{ \varepsilon_1 \quad \varepsilon_2 \quad \varepsilon_3 \quad \varepsilon_4 \quad \varepsilon_5 \quad \varepsilon_6 \quad \varepsilon_7 \quad \varepsilon_8 \quad \varepsilon_9 \quad \varepsilon_{10} \}^{\mathrm{T}} \tag{5c}$$

The various submatrices involved in Eqs. (5b) and (5c) are given in Appendix A.

The thermal strain vector $\{\bar{\varepsilon}_{\mathrm{t}}\}$ is represented as

$$\{\bar{\varepsilon}_{\mathrm{t}}\} = \left\{ \begin{array}{c} \bar{\varepsilon}_{xx} \\ \bar{\varepsilon}_{yy} \\ \bar{\varepsilon}_{zz} \\ \bar{\varepsilon}_{xy} \\ \bar{\varepsilon}_{xz} \\ \bar{\varepsilon}_{yz} \end{array} \right\} = \Delta T \left\{ \begin{array}{c} \alpha_x \\ \alpha_y \\ \alpha_z \\ \alpha_{xy} \\ 0 \\ 0 \end{array} \right\} \tag{5d}$$

where ΔT is the rise in temperature and is generally represented as function of x, y, and z. α_x, α_y, α_z and α_{xy} are thermal expansion coefficients in the shell co-ordinates and can be related to the thermal coefficients (α_1, α_2 and α_3) in the material principal directions.

The constitutive relations for an arbitrary layer k, in the laminated shell (x, y, z) co-ordinate system can be expressed as

$$\{\sigma\} = \begin{Bmatrix} \sigma_{xx} \\ \sigma_{yy} \\ \sigma_{zz} \\ \tau_{xy} \\ \tau_{xz} \\ \tau_{yz} \end{Bmatrix} = [\bar{C}^k]\{\varepsilon\} = \begin{bmatrix} \bar{C}_{11} & \bar{C}_{12} & \bar{C}_{13} & \bar{C}_{14} & 0 & 0 \\ \bar{C}_{12} & \bar{C}_{22} & \bar{C}_{23} & \bar{C}_{24} & 0 & 0 \\ \bar{C}_{13} & \bar{C}_{23} & \bar{C}_{33} & \bar{C}_{34} & 0 & 0 \\ \bar{C}_{14} & \bar{C}_{24} & \bar{C}_{34} & \bar{C}_{44} & 0 & 0 \\ 0 & 0 & 0 & 0 & \bar{C}_{55} & \bar{C}_{56} \\ 0 & 0 & 0 & 0 & \bar{C}_{56} & \bar{C}_{66} \end{bmatrix}^k \begin{Bmatrix} \varepsilon_{xx} - \bar{\varepsilon}_{xx} \\ \varepsilon_{yy} - \bar{\varepsilon}_{yy} \\ \varepsilon_{zz} - \bar{\varepsilon}_{zz} \\ \gamma_{xy} - \bar{\gamma}_{xy} \\ \gamma_{xz} - \bar{\gamma}_{xz} \\ \gamma_{yz} - \bar{\gamma}_{yz} \end{Bmatrix} \tag{6}$$

where the elements of the stiffness coefficients, $\bar{C}^k_{ij}$ $(i, j = 1, 6)$ can be obtained using the appropriate transformation on the stiffness matrix $[C_k]$ corresponding to material principal directions, as outlined in the literature (Herakovich, 1998). $\{\sigma\}$, $\{\varepsilon\}$ and $\{\bar{\varepsilon}_t\}$ are stress, strain, and thermal strain vectors due to rise in temperature, respectively.

The governing equations for the shell structure are obtained by applying Lagrangian equations of motion given by

$$\frac{\mathrm{d}}{\mathrm{d}t}[\partial(T - U_T)/\partial\dot{\delta}_i] - [\partial(T - U_T)/\partial\delta_i] = 0, \quad i = 1, \ldots, n \tag{7}$$

where T is the kinetic energy; U_T is the total potential energy consisting of strain energy contributions due to the in-plane and transverse stresses, and work done by the externally applied mechanical loads, respectively. $\{\delta\} = \{\delta_1, \delta_2, \ldots, \delta_i, \ldots, \delta_n\}^T$ is the vector of generalized displacements and δ_i are independent. A dot over the variables represents the partial derivative with respect to time. The superscript T refers the transpose of a matrix/vector.

The kinetic energy of the shell is given by

$$T(\delta) = \frac{1}{2}\int\int\left[\sum_{k=1}^{n}\int_{h_k}^{h_{k+1}} \rho_k \{\dot{u}^k \quad \dot{v}^k \quad \dot{w}^k\}\{\dot{u}^k \quad \dot{v}^k \quad \dot{w}^k\}^T\left(1 + \frac{z}{R}\right)\mathrm{d}z\right]\mathrm{d}x\,\mathrm{d}y \tag{8}$$

where ρ_k is the mass density of the kth layer. h_k, h_{k+1} are the z co-ordinates of laminate corresponding to the inner and outer surfaces of the kth layer.

Using the kinematics given in Eq. (1), Eq. (8) can be rewritten as

$$T(\dot{\delta}) = \frac{1}{2}\int\int\left[\sum_{k=1}^{n}\int_{h_k}^{h_{k+1}} \rho_k \{\dot{d}\}^T[Z]^T[Z]\{\dot{d}\}\left(1 + \frac{z}{R}\right)\mathrm{d}z\right]\mathrm{d}x\,\mathrm{d}y \tag{9}$$

where

$$\{\dot{d}\}^T = \{\dot{u}_0 \quad \dot{v}_0 \quad \dot{w}_0 \quad \dot{\theta}_x \quad \dot{\theta}_y \quad \dot{w}_1 \quad \dot{\beta}_x \quad \dot{\beta}_y \quad \dot{\Gamma} \quad \dot{\phi}_x \quad \dot{\phi}_y \quad \dot{\psi}_x \quad \dot{\psi}_y\}$$

and

$$[Z] = \begin{bmatrix} 1 & 0 & 0 & z & 0 & 0 & z^2 & 0 & 0 & z^3 & 0 & S^k & 0 \\ 0 & 1 & 0 & 0 & z & 0 & 0 & z^2 & 0 & 0 & z^3 & 0 & S^k \\ 0 & 0 & 1 & 0 & 0 & z & 0 & 0 & z^2 & 0 & 0 & 0 & 0 \end{bmatrix}$$

The potential energy functional U_T is given by,

$$U_T(\delta) = \frac{1}{2}\int\int\left[\sum_{k=1}^{n}\int_{h_k}^{h_{k+1}}\{\sigma\}^T\{\varepsilon\}\left(1+\frac{z}{R}\right)dz\right]dx\,dy - \int\int qw\,dx\,dy \tag{10}$$

where q is the distributed force acting on the inner surface of the shell.

Using Eqs. (5a)–(5d), and (6), the potential energy functional U_T given by Eq. (10) can be rewritten as

$$U_T(\delta) = \frac{1}{2}\int\int\left[\sum_{k=1}^{n}\int_{h_k}^{h_{k+1}}(\{\bar{\varepsilon}\}^T[\bar{Z}]^T[\bar{C}^k][\bar{Z}]\{\bar{\varepsilon}\} - 2\{\bar{\varepsilon}\}^T[\bar{Z}]^T[\bar{C}^k]\{\bar{\varepsilon}_t\} + \{\bar{\varepsilon}_t\}^T[\bar{C}^k]\{\bar{\varepsilon}_t\})\left(1+\frac{z}{R}\right)dz\right]dx\,dy - \int\int qw\,dx\,dy \tag{11}$$

The governing equations obtained by substituting Eqs. (9) and (11) in Eq. (7) can be solved analytically/numerically.

Here, finite element approach, using an eight-noded quadrilateral shell element having thirteen degrees of freedoms/generalized displacements per node ($\{\delta_i^e\} = \{u_0^i, v_0^i, w_0^i, \theta_x^i, \theta_y^i, w_1^i, \beta_x^i, \beta_y^i, \Gamma^i, \phi_x^i, \phi_y^i, \psi_x^i, \psi_y^i\}^T$ for ith node) is adopted for solving the governing equations. To obtain the kinetic and the total potential energies for the element, the vector $\{\dot{d}\}$ and the strain vector $\{\bar{\varepsilon}\}$ involved in Eqs. (9) and (11) are expressed in terms of shape/interpolation functions, their derivatives (Zienkiewicz, 1971), and the vector of element level degrees of freedoms/generalized displacements $\{\delta^e\}$ as

$$\{\dot{d}\}_{13x1} = [H]_{13x104}\{\dot{\delta}^e\}_{104x1}; \quad \{\bar{\varepsilon}\}_{35x1} = [B]_{35x104}\{\delta^e\}_{104x1} \tag{12}$$

where

$$\{\delta^e\} = \{\,\{\delta_1^e\}^T \quad \{\delta_2^e\}^T \quad \{\delta_3^e\}^T \quad \{\delta_4^e\}^T \quad \{\delta_5^e\}^T \quad \{\delta_6^e\}^T \quad \{\delta_7^e\}^T \quad \{\delta_8^e\}^T\,\}$$

The kinetic and the total potential energy expressions, simplified using Eq. (12), are given as

$$T(\delta^e) = \frac{1}{2}\{\dot{\delta}^e\}^T[M^e]\{\dot{\delta}^e\} \tag{13}$$

$$U_T(\delta^e) = \frac{1}{2}\{\delta^e\}^T[K^e]\{\delta^e\} - \{\delta^e\}^T\{F_T^e\} - \{\delta^e\}^T\{F_M^e\} + \frac{1}{2}\int\int\left[\sum_{k=1}^{n}\int_{h_k}^{h_{k+1}}\{\bar{\varepsilon}_t\}^T[\bar{C}^k]\{\bar{\varepsilon}_t\}\left(1+\frac{z}{R}\right)dz\right]dx\,dy \tag{14}$$

The elemental governing equations, obtained by substituting Eqs. (13) and (14) in Eq. (7), are

$$[M^e]\{\ddot{\delta}^e\} + [K^e]\{\delta^e\} = \{F_T^e\} + \{F_M^e\} \tag{15}$$

where the elemental mass $[M^e]$ and stiffness $[K^e]$ matrices, and thermal/mechanical load vectors ($\{F_T^e\}$ and $\{F_M^e\}$) can be expressed as

$$\begin{aligned}
[M^e] &= \int\int\left[\sum_{k=1}^{n}\int_{h_k}^{h_{k+1}}\rho\{H\}^T[Z]^T[Z]\{H\}\left(1+\frac{z}{R}\right)dz\right]dx\,dy\\
[K^e] &= \int\int\left[\sum_{k=1}^{n}\int_{h_k}^{h_{k+1}}[B]^T[\bar{Z}]^T[\bar{C}^k][\bar{Z}][B]\left(1+\frac{z}{R}\right)dz\right]dx\,dy\\
\{F_T^e\} &= \int\int\left[\sum_{k=1}^{n}\int_{h_k}^{h_{k+1}}[B]^T[\bar{Z}]^T[\bar{C}^k]\{\bar{\varepsilon}_t\}\left(1+\frac{z}{R}\right)dz\right]dx\,dy
\end{aligned} \tag{16}$$

and

$$\{F_{\mathrm{M}}^{\mathrm{e}}\} = \int\int \{H_w\}^{\mathrm{T}} q \, \mathrm{d}x \, \mathrm{d}y$$

The coefficients of mass and stiffness matrices, and the load vectors involved in governing Eq. (15) can be rewritten as the product of term having thickness co-ordinate z alone and the term containing x and y. In the present study, while performing the integration, terms having thickness co-ordinate z are explicitly integrated whereas the terms containing x and y are evaluated using full integration with 5×5 points Gauss integration rule. Following the usual finite element assembly procedure (Zienkiewicz, 1971), the governing equation for the forced response of the laminated shell are obtained as

$$[M]^{\mathrm{G}}\{\ddot{\delta}\}^{\mathrm{G}} + [K]^{\mathrm{G}}\{\delta\}^{\mathrm{G}} = \{F_{\mathrm{T}}\}^{\mathrm{G}} + \{F_{\mathrm{M}}\}^{\mathrm{G}} \tag{17}$$

where $[M^{\mathrm{G}}]$ and $[K^{\mathrm{G}}]$ are the global mass and stiffness matrices. $\{F_{\mathrm{T}}\}^{\mathrm{G}}$, $\{F_{\mathrm{M}}\}^{\mathrm{G}}$ are the global thermal and mechanica load vectors, respectively. $\{\ddot{\delta}\}^{\mathrm{G}}$ and $\{\delta\}^{\mathrm{G}}$ are the global acceleration and displacement vectors respectively.

The solutions of Eq. (17) can be obtained using Newmark's direct time integration method (Subbaraj and Dokainish, 1989).

3. Element description

The element employed here is a simple C^0 continuous, shear flexible and serendipity type of quadrilateral shell element (HSDT13) with 13 nodal degrees of freedom as outlined in the formulation. It is developed based on field consistency approach (Pratap, 1985).

If the interpolation functions for an eight-noded element are used directly to interpolate the thirteen field variables (u_0, v_0, w_0, θ_x, θ_y, w_1, β_x, β_y, Γ, ϕ_x, ϕ_y, ψ_x, ψ_y) in deriving the membrane and shear strains, the element will lock and show oscillation in the membrane and shear stresses. Field consistency requires that the membrane and the transverse shear strains must be interpolated in a consistent manner. Thus, the w_0 term in the expression for membrane strain $\{\varepsilon_1\}$ (second strain component) given in Eq. (A.2) have to be consistent with the field functions $v_{0,y}$. Similarly, the terms θ_x and (θ_y, v_0) in the expression for transverse shear strains ($\{\varepsilon_6\}$ and $\{\varepsilon_{10}\}$) given in Eq. (A.3) have to be consistent with the field functions $w_{0,x}$ and $w_{0,y}$, respectively, as outlined in the work of Pratap (1985). This is achieved by using a field-redistributed substitute shape functions to interpolate those specific terms that must be consistent. The element thus derived is tested for its basic properties and is found free from the rank deficiency, shear/membrane locking, and poor convergence syndrome. For the sake of brevity, the development of the element based on such displacement approximation, and its performances are omitted, as they are available in the literature (Ganapathi and Makhecha, 2001; Makhecha et al., 2001a; Makhecha et al., 2001b; Makhecha et al., 2001c; Ganapathi et al., 2002) and it follows the standard procedure for the given kinematics and structural theory. The element HSDT13 is applicable for both thick and thin situations.

The finite element represented as per the kinematics given in Eq. (1), is referred as HSDT13. Five more alternate standard discrete models are proposed, to study the influence of higher-order terms in the displacement functions, whose displacement fields are deduced from the original element by deleting the appropriate degrees of freedom (w_1 and $\Gamma = 0$; or $\psi = 0$; or ψ, w_1 and $\Gamma = 0$; or z^2 terms, ψ, w_1 and $\Gamma = 0$; or dropping all the higher-order terms). These alternate models, and the corresponding nodal degrees of freedom are shown in Table 1.

Table 1
Alternate eight-noded finite element models considered for parametric study

Finite element model	Degrees of freedom per node
HSDT13 (Present)	u_0, v_0, w_0, θ_x, θ_y, w_1, β_x, β_y, Γ, ϕ_x, ϕ_y, ψ_x, ψ_y
HSDT11a	u_0, v_0, w_0, θ_x, θ_y, β_x, β_y, ϕ_x, ϕ_y, ψ_x, ψ_y
HSDT11b	u_0, v_0, w_0, θ_x, θ_y, w_1, β_x, β_y, Γ, ϕ_x, ϕ_y
HSDT9	u_0, v_0, w_0, θ_x, θ_y, β_x, β_y, ϕ_x, ϕ_y
HSDT7	u_0, v_0, w_0, θ_x, θ_y, ϕ_x, ϕ_y
FSDT5	u_0, v_0, w_0, θ_x, θ_y

4. Results and discussion

The study, here, is mainly focused on dynamic response analysis of simply supported non-circular cross-ply cylindrical shells, with elliptical cross-section, subjected to thermal/mechanical loads, considering various higher-order theories possible within the scope of assumed kinematics employed in the formulation. Since the higher-order theory, in general, is required for the accurate analysis of thick composite structures, the emphasis in the present work is placed on the laminated shells with radius-to-thickness ratios $\leqslant 50$. For the detailed parametric study, the shear correction factor is taken as 5/6 for the first-order model. Furthermore, the influences of various parameters such as radius-to-thickness (R_0/h) and length-to-radius (L/R_0) ratios, eccentricity ($\varepsilon = [1-(b/a)^2]^{1/2}$) and number of layers ($N$) on the response characteristics of shells are analyzed. Further, all the strain energy terms are evaluated using exact numerical integration scheme as the element employed is based on the field consistency approach.

Based on the progressive mesh refinement, a 16×8 grid mesh (circumferential and meridional directions) is found to be adequate to model the one-eighth of the shells (quarter in cross-section and half in length) for the present analysis. Before proceeding for the detailed study, the formulation developed herein is validated considering the free vibration of laminated cross-ply circular and elliptical cylindrical shells against analytical/three-dimensional solutions (Ye and Soldatos, 1997; Suzuki et al., 1996; ANSYS, 1997) and they are shown in Tables 2 and 3. For the validation purpose, the value for the shear correction factor is assumed as 1 in the present FSDT5 as the same value is assumed in the FSDT model of Suzuki et al. (1996). It may be noted here that the solutions obtained for the elliptical case using present FSDT5 agree well with those of analytical approach (Suzuki et al., 1996). However, it is seen from these tables that the results of present model HSDT13 agree well with the three-dimensional solutions. For the dynamic response analysis, the solutions obtained using the present formulation agree very well with the available numerical results, based on the classical theory, for an isotropic case (Cheung et al., 1991). For the sake of brevity, these results are not presented.

Table 2
Verification of present results with 3D elasticity solutions for natural frequency parameter Ω ($= \omega R\sqrt{\rho/E_2}$) of a simply-supported cross-ply circular cylindrical shell

Circumferential wave number, n	R/h					
	5		10		20	
	HSDT13	3D analytical solution (Ye and Soldatos, 1997)	HSDT13	3D analytical solution (Ye and Soldatos, 1997)	HSDT13	3D analytical solution (Ye and Soldatos, 1997)
1	0.339297	0.339	0.331522	0.332	0.329408	0.329
2	0.306985	0.306	0.224928	0.225	0.197009	0.197
3	0.594289	0.591	0.330063	0.329	0.194639	0.194

0°/90°/0°, $E_1/E_2 = 25$; $L/R = 5$; Longitudinal mode number, $m = 1$.

Table 3
Comparison of different models with analytical/3D FEM solutions for frequency parameter ($\bar{\Omega}^2$)[a] of cross-ply elliptical shell

L/R_0	Theory	SS modes		AA modes		SA modes			AS modes		
		First	Second	First	Second	First	Second	Third	First	Second	Third
6.2832	FSDT5[b]	0.1658	3.0450	0.2265	3.0557	0.0624	1.0251	6.3913	0.0333	1.023	6.3814
	FSDT[b,c]	0.167	3.054	0.227	3.066	0.063	1.029	–	0.034	1.028	–
	HSDT7	0.1552	2.5913	0.2169	2.6015	0.0624	0.9087	5.2874	0.0333	0.9077	5.2829
	HSDT9	0.1551	2.5912	0.2169	2.6014	0.0623	0.9087	5.2873	0.0333	0.9076	5.2828
	HSD-T11b	0.1488	2.5620	0.2139	2.5750	0.0624	0.8902	5.2539	0.0333	0.8932	5.2516
	HSD-T11a	0.1523	2.4921	0.2144	2.5021	0.0623	0.8804	5.0691	0.0333	0.8796	5.0654
	HSD-T13	0.1461	2.4654	0.2116	2.4779	0.0624	0.8637	5.0393	0.0333	0.8661	5.0376
	3D FEM[d]	0.1454	2.4498	0.2096	2.4571	0.0623	0.8581	5.0064	0.0332	0.8563	5.0006
1.0472	FSDT5[b]	1.1216	3.8628	1.2612	3.8996	1.7681	3.4298	7.2371	1.4162	2.0683	7.2364
	FSDT[b,c]	1.144	3.909	1.285	–	1.800	3.446	7.308	1.439	2.098	–
	HSDT7	1.1014	3.3671	1.2388	3.4063	1.6342	3.4189	6.0731	1.3707	1.9697	6.0730
	HSDT9	1.0995	3.3634	1.2364	3.4022	1.6318	3.4157	6.0689	1.3698	1.9661	6.0687
	HSD-T11b	1.0911	3.3328	1.2295	3.3741	1.6130	3.413	6.0382	1.3626	1.9521	6.0401
	HSD-T11a	1.0943	3.2536	1.2304	3.2927	1.5987	3.4132	5.8368	1.3567	1.9441	5.8363
	HSD-T13	1.0863	3.2254	1.2238	3.2668	1.5811	3.4107	5.8092	1.3510	1.9312	5.8106
	3D FEM[d]	1.0827	3.209	1.2191	3.245	1.5749	3.4033	5.7749	1.3453	1.9222	5.7727

90°/0°/90°; $R_0/h = 6$, $a/b = 1.53$ ($\varepsilon = 0.7568$); $E_1/E_2 = 15.40$, $G_{12}/E_2 = 0.7924$, $G_{23}/E_2 = 0.3850$, $E_2 = 8.96$ GPa, $\nu_{12} = 0.3$; S: Symmetric, A: Antisymmetric.

[a] $(\bar{\Omega}^2) = \rho_0\omega^2 R_0^2\{12(1-\nu_{13}\nu_{21})\}/E_1$.

[b] Shear correlation factor = 1.0.

[c] Suzuki et al. (1996).

[d] ANSYS (1997) (20 noded solid element; Mesh: $20 \times 40 \times 20$ on 1/8th model).

For the transient response study, all the initial conditions are assumed to be zero. The critical time step of a conditionally stable finite difference scheme is introduced as a guide (Leech, 1965; Tsui and Tong, 1971) in the present study. Subsequently, a convergence study is conducted to select a time step, which yields an accurate solution. The responses of displacements along the circumferential and transverse directions (v and w) are depicted here corresponding to the (x, y, z) locations of ($L/2$, $C/4$, $h/2$), and ($L/2$, 0, $h/2$), respectively. Here, C denotes the complete circumferential length of elliptical shell. The material properties used, unless otherwise mentioned, are $E_1/E_2 = 40$, $G_{12}/E_2 = G_{13}/E_2 = 0.6$, $G_{23}/E_2 = 0.5$, $\nu_{12} = \nu_{23} = \nu_{13} = 0.25$, $\alpha_2/\alpha_1 = \alpha_3/\alpha_1 = 1125$, $E_2 = E_3 = 10^9$ N/m^2, $\alpha_1 = 10^{-5}$ °C^{-1}, $\rho = 1500$ kg/m^3, where E, G, ν and ρ are Young's modulus, shear modulus, Poisson's ratio and density. The subscripts 1, 2 and 3 refer to the principal material directions. All the layers are of equal thickness and the ply-angle is measured with respect to the x-axis (meridional axis). The spatial distributions of loading considered here are—for thermal case: $\Delta T = T_0(2z/h)\sin(\pi x/L)\cos(6\pi y/C)$; for internal pressure loading case: $q = q_0\sin(\pi x/L)\cos(6\pi y/C)$.

The details of boundary conditions used are:

Simply supported edges:

$$v_0 = w_0 = \theta_y = w_1 = \beta_y = \Gamma = \phi_y = \psi_y = 0 \quad \text{at } x = 0, L$$

Along the lines of symmetry:

$$u_0 = \theta_x = \beta_x = \phi_x = \psi_x = 0 \quad \text{at } x = L/2$$

$$v_0 = \theta_x = \beta_x = \phi_x = \psi_x = 0 \quad \text{at } y = 0$$

Along the line of anti-symmetry:

$$u_0 = w_0 = \theta_x = w_1 = \beta_x = \Gamma = \phi_x = \psi_x = 0 \quad \text{at } y = C/4$$

Firstly, the dynamic thermal response analysis is carried out considering two-layered unsymmetric thick elliptical shells [$L/R_0 = 0.5$, $R_0/h = 5$, $a/b = 1.25$ and 2.5 ($\varepsilon = 0.6$ and 0.9165), $h = 0.001$ m, (0°/90°)] subjected to thermal load ($T_0 = 1$). The variations of the transverse (w/h) and in-plane (v/h) displacements with time predicted by different models, as outlined in Table 1, are presented in Fig. 2. It is observed from Fig. 2 that the maximum amplitudes given using FSDT5 and HSDT7 are very low, and moderately low by HSDT9 and HSDT11a when compared with those of HSDT11b and HSDT13. Although model HSDT7 appear to be similar to that of HSDT9, there is a noticeable discrepancy in the results between them. This is attributed to the insufficient representation of membrane response in HSDT7 for the unsymmetric laminates i.e. missing even power terms in z in the in-plane displacements. Furthermore, the response characteristics, in particular, transverse displacement calculated by HSDT11b matches very well with that of HSDT13 and both exhibit high frequency oscillations because of the participation of thickness stretch

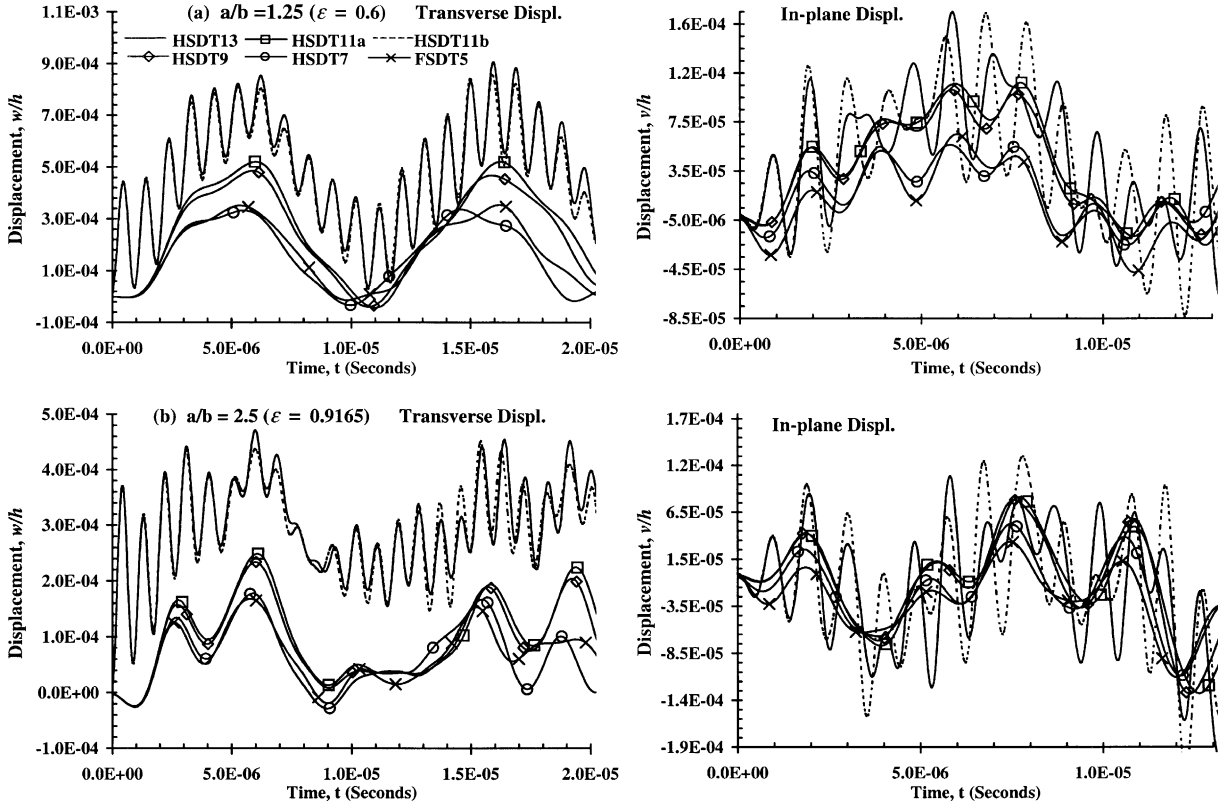

Fig. 2. Transverse and in-plane displacements (w and v) responses of two-layered cross-ply (0°/90°) elliptical cylindrical shells ($L/R_0 = 0.5$, $R_0/h = 5$) subjected to thermal load (a) $a/b = 1.25$ ($\varepsilon = 0.6$) and (b) $a/b = 2.5$ ($\varepsilon = 0.9165$).

modes captured due to the presence of Γ term in the kinematics. It can be noted here that Bhaskar et al. (1996) have highlighted the importance of thickness-stretch effect while dealing with the three-dimensional thermo-elastic analysis of thick laminates. It is further seen from the performances of HSDT11a and HSDT9 as well as HSDT13 and HSDT11b that the introduction of zigzag terms (ψ) in in-plane displacement descriptions does not affect appreciably the transverse response behavior. It is also noticed that, with the increase in the value of the eccentricity parameter (ε), the nature of the periodic oscillation changes due to the profound participation of many circumferential modes and the rate of difference in maximum amplitude shown by HSDT13/HSDT11b with other models also increases, even for a fairly thin shell case (see Fig. 3). It is further seen that, with the increase in eccentricity parameter, the maximum response level decreases due to the increase in the stiffness of the shells. In the case of the in-plane displacement along the circumferential direction (Fig. 2), the response characteristics are somewhat qualitatively similar to those of transverse motion but the rate of variation in the peak amplitude evaluated by various models, and the influence of thickness stretching mode are, in general, less in comparison with that of the transverse motion. However, for the in-plane response case, the interaction of the thickness stretch mode (Γ) and slope discontinuity (ψ) affects the response as highlighted by the performance of HSDT11b and HSDT13.

Next, for a shell with fairly high eccentricity parameter ($\varepsilon = 0.9165$, which corresponds to $a/b = 2.5$) considered here, the influence of number of layers on the dynamic characteristics obtained using present model (HSDT13) is examined along with the performances of the standard models (HSDT11b, HSDT7 and FSDT5) employed for the free vibration study in the literature (Noor, 1973; Suzuki et al., 1996; Kumar and Singh, 1995; Soldatos, 1987) and are depicted in Fig. 4. For clarity, the results of HSDT11b are not shown here as it almost follows the pattern of HSDT13. The present model shows distinctly different displacement oscillation with higher amplitudes. It is evident from Figs. 2 (b) and 4 (b) that, with increase in number of layers, the amplitude of the response decreases as expected due to the weakening of bending-stretching

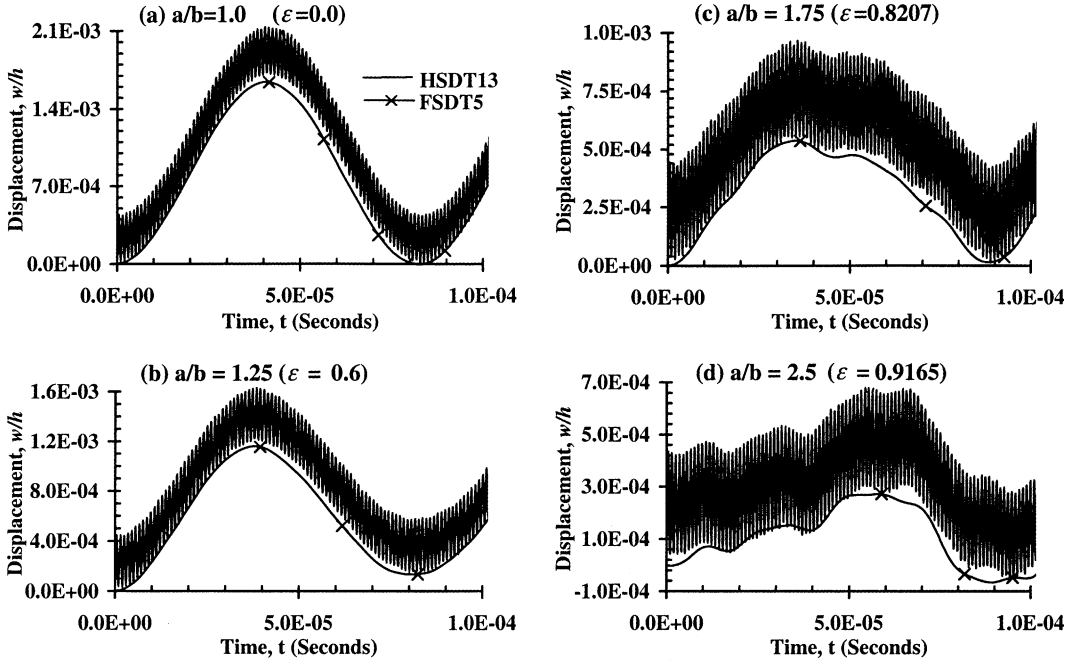

Fig. 3. The effect of eccentricity parameter (ε) on the transverse displacement (w) for eight-layered cross-ply elliptical cylindrical shells ($L/R_0 = 0.5$, $R_0/h = 25$, $(0°/90°)_4$) subjected to thermal loading.

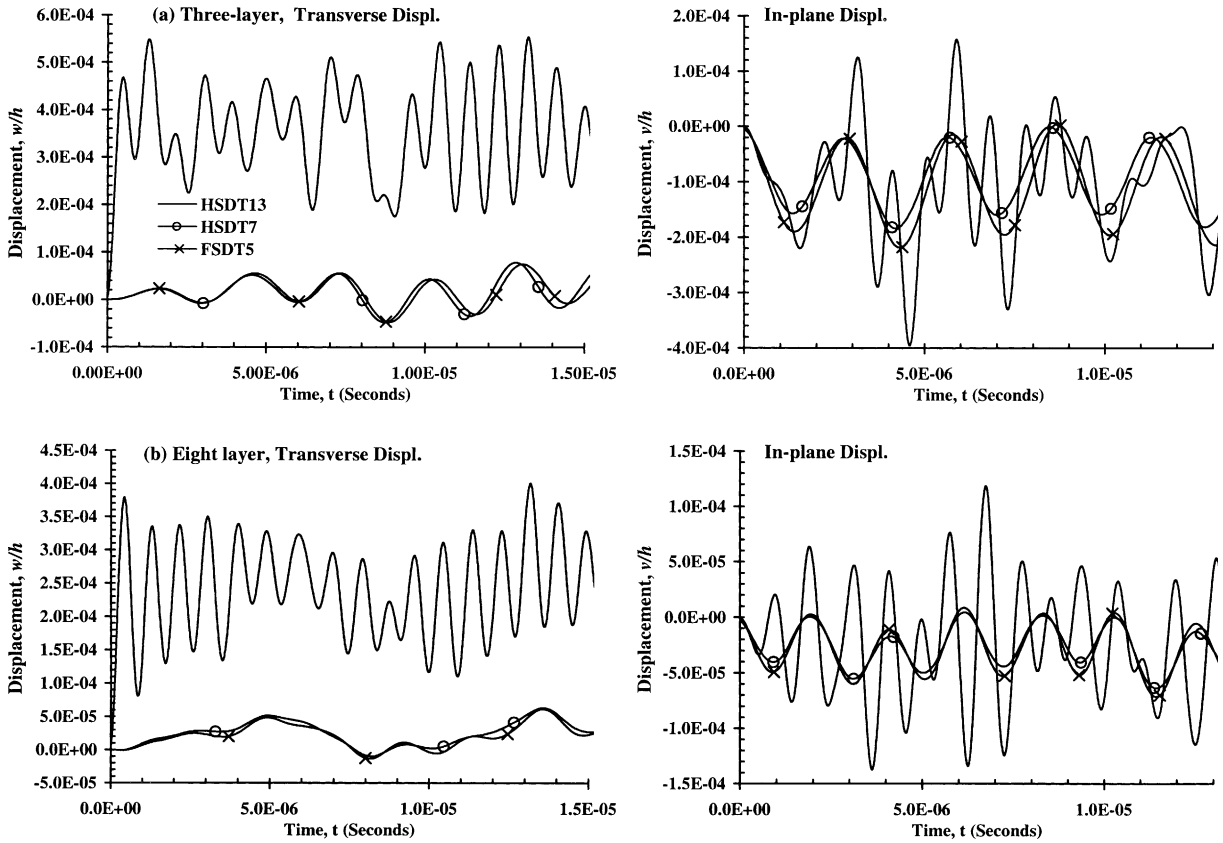

Fig. 4. The effect of number of layers on the displacements (w, v) for the elliptical cylindrical shell ($a/b = 2.5$ ($\varepsilon = 0.9165$), $L/R_0 = 0.5$, $R_0/h = 5$) subjected to thermal loading: (a) three-layer (0°/90°/0°) and (b) eight-layer $(0°/90°)_4$.

couplings and the participation of different circumferential modes appears to be less. However, it is inferred that the effect of the directional stiffnesses, provided by symmetric/unsymmetric lay-up can influence the response pattern.

Fig. 5 highlights the influences of radius-to-thickness and length-to-radius ratios on the dynamic behavior of elliptical shells. It can be viewed that, for a fairly short shell considered here ($L/R_0 = 0.5$), the effect of thickness stretching mode on the variation of the displacement with time decreases with the increase in the value of R_0/h. However, the model HSDT13 predicts distinctly different response in comparison with those of FSDT5 even for a fairly thin shell of $R_0/h = 50$ but the discrepancy in the results between these theories is considerably less, as expected. It is also observed from Fig. 5 that, for a long shell ($L/R_0 = 5$), the interaction of thickness stretching mode on the response is noticeable only when the shell is very thick. Furthermore, it reveals that, with increase in R_0/h, the discrepancy in the results obtained using higher- and first-order theories, decreases rapidly for long shell compared to those of short one. It can be further opined that, in general, HSDT11b model can closely approximate the complete model HSDT13 for accurately yielding the characteristics of multi-layered short thick shells as well as fairly thin shell under thermal loads.

Similar studies are conducted for the response characteristics of shell subjected to internal pressure ($q_0 = 100$ N/m^2) through various structural models. For the sake of clarity, the results pertaining to FSDT5

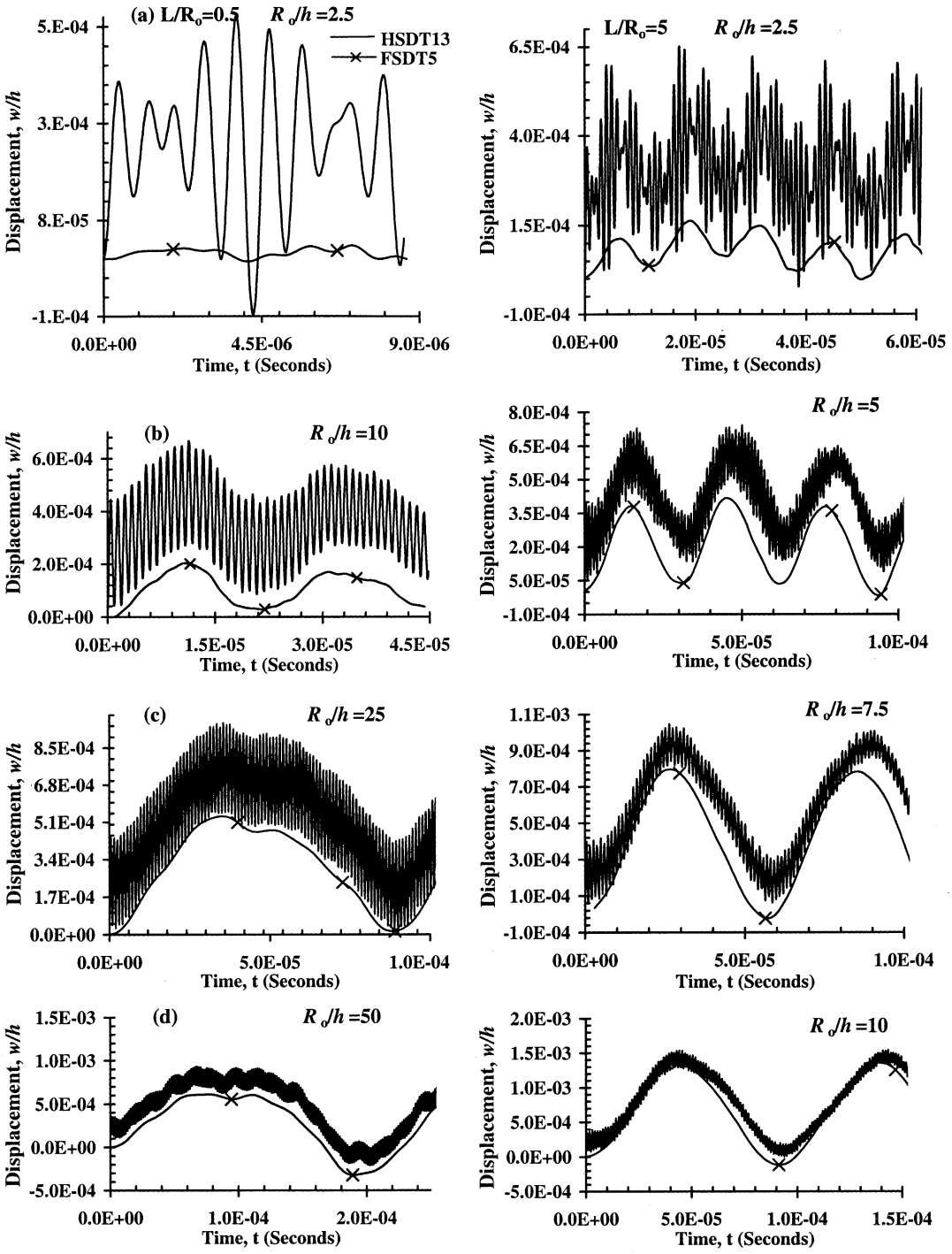

Fig. 5. The influence of thickness ratio on the transverse displacement (w) response for the elliptical cylindrical shells $((0°/90°)_4$, $a/b = 1.75$ ($\varepsilon = 0.8207$)) subjected to thermal load: (a) $L/R_0 = 0.5$ (left side) and (b) $L/R_0 = 5$ (right side).

and HSDT7 are omitted from the plots as they under estimate the response values like in the case of thermal loads. The results obtained for the two-layered elliptical shells [$L/R_0 = 0.5$, $R_0/h = 5$, $a/b = 1.25$ and 2.5 ($\varepsilon = 0.6$ and 0.9165), 0°/90°] are described in Fig. 5. It is noticed that the differences in the initial response evaluated among various models are less. However, with the increase in the response time, the variation of displacement patterns depends on the type of model employed. It is further inferred that some reduction in the peak amplitude and shift in the response period are shown from the performance of different models. It is seen that the response periods predicted by models HSDT9 and HSDT11b are almost same whereas the models HSDT11a and HSDT13 yield nearly similar behavior. Although the effect of thickness stretching mode is to introduce high frequency oscillations in the response, the intensity is very less compared to those of thermal case. In general, it can be argued while studying the mechanical load case that the model having zigzag variation in the in-plane displacement (HSDT11a) can approximate to some extent the complete model (Fig. 6).

The effect of thickness and length ratios on the response of shells with internal pressure is highlighted in Fig. 7. It is evident from this Figure that, for short shells, the influence of higher-order model rapidly decreases with the increase in the thickness ratio in comparison with those of thermal case whereas it makes little difference for the long shell case, even for the thick situation.

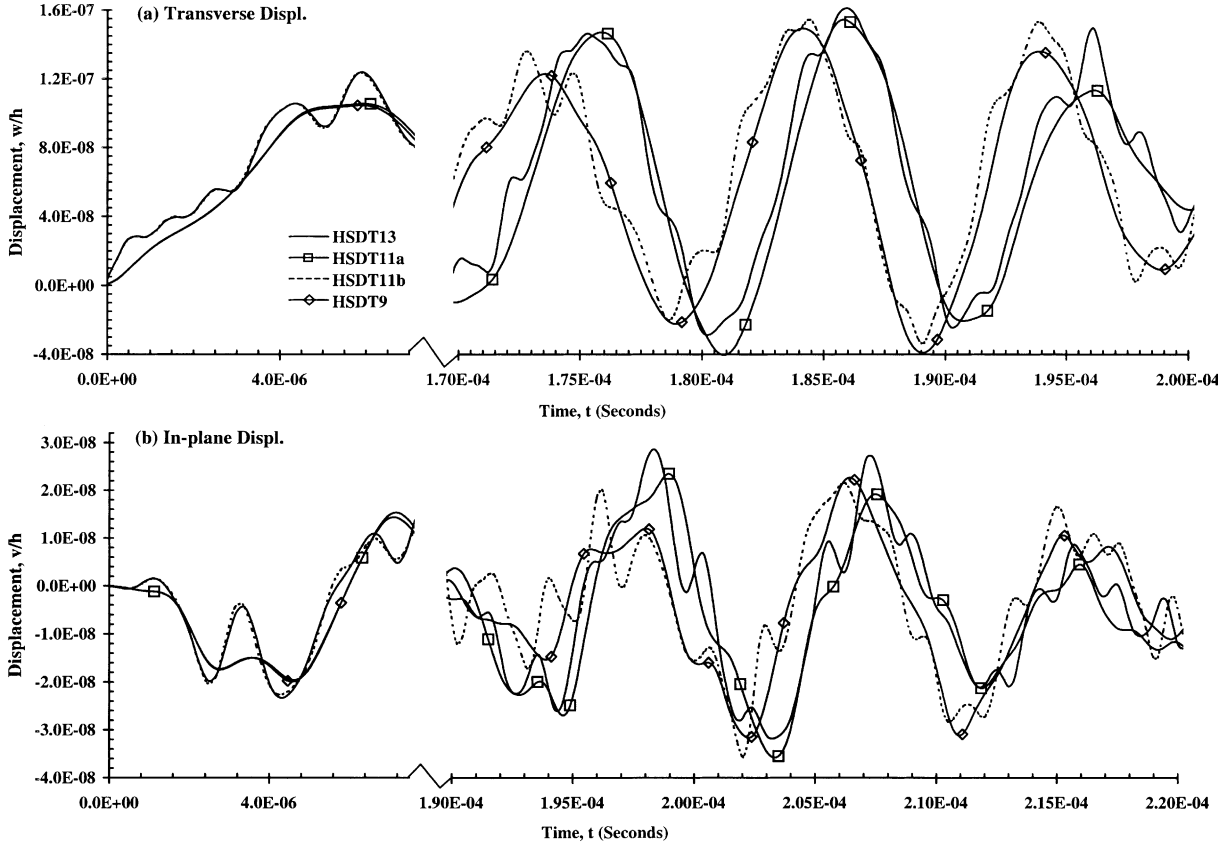

Fig. 6. Transverse and in-plane displacements (w and v) responses of two-layered cross-ply (0°/90°) elliptical cylindrical shells ($a/b = 1.25$ ($\varepsilon = 0.6$), $L/R_0 = 0.5$, $R_0/h = 5$) subjected to internal pressure loading.

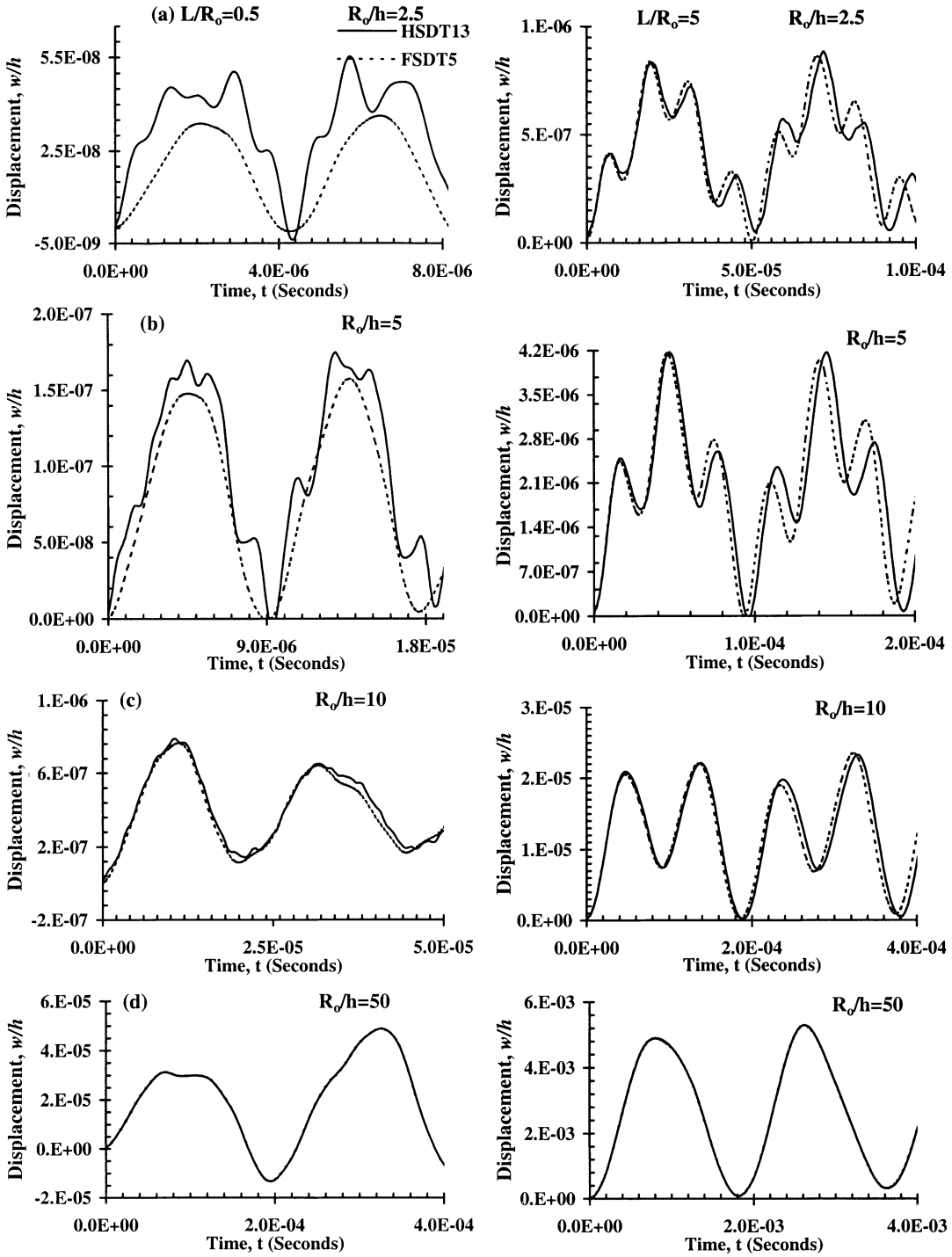

Fig. 7. The influence of thickness ratio on the displacement (w) for the elliptical cylindrical shell $((0°/90°)_4$; $a/b = 1.75$ ($\varepsilon = 0.8207$)) under internal pressure: (a) $L/R_0 = 0.5$ (left side); (b) $L/R_0 = 5$ (right side).

5. Conclusions

The effectiveness of the present formulation (HSDT13) is demonstrated considering dynamic analysis of thick laminated cross-ply elliptical shells subjected to thermal and mechanical loads. Parametric studies are made to provide some insight into the effects of variations in the degree of non-circularity, length and thickness ratios on the response characteristics of cylinders. The performance of other possible higher-order models is also brought out. The inclusion of thickness stretching terms (Γ) in the transverse displacement field is essential for the thermal response study compared to the slope discontinuity terms (ψ) in the in-plane displacement functions. For the mechanical loading case, both the ψ and Γ in the displacement fields are to some extent important in evaluating the response characteristics. It is also revealed that, for short/long shells under thermal load, the influence of higher-order model is considerable even for fairly thin situation whereas, for mechanical case, it is important for thick short shells.

Appendix A

The various submatrices involved in Eqs. (5b) and (5c) are

$$[Z_1]=\begin{bmatrix}1 & 0 & 0 & 0 & 0\\ 0 & \dfrac{1}{1+z/R} & 0 & 0 & 0\\ 0 & 0 & 1 & 0 & 0\\ 0 & 0 & 0 & \dfrac{1}{1+z/R} & 1\end{bmatrix};\quad [Z_2]=z[Z_1];\quad [Z_3]=\begin{bmatrix}z^2 & 0 & 0 & 0\\ 0 & \dfrac{z^2}{1+z/R} & 0 & 0\\ 0 & 0 & 0 & 0\\ 0 & 0 & \dfrac{z^2}{1+z/R} & z^2\end{bmatrix};$$

$$[Z_4]=z[Z_3];\quad [Z_5]=\begin{bmatrix}S^k & 0 & 0 & 0\\ 0 & \dfrac{S^k}{1+z/R} & 0 & 0\\ 0 & 0 & 0 & 0\\ 0 & 0 & \dfrac{S^k}{1+z/R} & S^k\end{bmatrix};\quad [Z_6]=\begin{bmatrix}1 & 0\\ 0 & 1\end{bmatrix};\quad [Z_7]=z[Z_6];\quad [Z_8]=z^2[Z_6];$$

$$[Z_9]=S^k_{,z}[Z_6];\quad [Z_{10}]=\begin{bmatrix}0 & 0 & 0 & 0 & 0\\ \dfrac{1}{1+z/R} & \dfrac{z}{1+z/R} & \dfrac{z^2}{1+z/R} & \dfrac{z^3}{1+z/R} & \dfrac{S^k}{1+z/R}\end{bmatrix} \tag{A.1}$$

$$\{\varepsilon_1\}=\begin{Bmatrix}u_{0,x}\\ v_{0,y}+\frac{w_0}{R}\\ w_1\\ u_{0,y}\\ v_{0,x}\end{Bmatrix};\quad \{\varepsilon_2\}=\begin{Bmatrix}\theta_{x,x}\\ \theta_{y,y}+\frac{w_1}{R}\\ 2\Gamma\\ \theta_{x,y}\\ \theta_{y,x}\end{Bmatrix};\quad \{\varepsilon_3\}=\begin{Bmatrix}\beta_{x,x}\\ \beta_{y,y}+\frac{\Gamma}{R}\\ \beta_{x,y}\\ \beta_{y,z}\end{Bmatrix};$$

$$\{\varepsilon_4\}=\begin{Bmatrix}\phi_{x,x}\\ \phi_{y,y}\\ \phi_{x,y}\\ \phi_{y,x}\end{Bmatrix};\quad \{\varepsilon_5\}=\begin{Bmatrix}\psi_{x,x}\\ \psi_{y,y}\\ \psi_{x,y}\\ \psi_{y,x}\end{Bmatrix} \tag{A.2}$$

$$\{\varepsilon_6\} = \begin{Bmatrix} \theta_x + w_{0,x} \\ \theta_y \end{Bmatrix}; \quad \{\varepsilon_7\} = \begin{Bmatrix} 2\beta_x + w_{1,x} \\ 2\beta_y \end{Bmatrix}; \quad \{\varepsilon_8\} = \begin{Bmatrix} 3\phi_x + \Gamma_{,x} \\ 3\phi_y \end{Bmatrix};$$

$$\{\varepsilon_9\} = \begin{Bmatrix} \psi_x \\ \psi_y \end{Bmatrix}; \quad \{\varepsilon_{10}\} = \begin{Bmatrix} w_{0,y} - \dfrac{v_0}{R} \\ w_{1,y} - \dfrac{\theta_y}{R} \\ \Gamma_{,y} - \dfrac{\beta_y}{R} \\ -\dfrac{\phi_y}{R} \\ -\dfrac{\psi_y}{R} \end{Bmatrix} \tag{A.3}$$

O_1 and O_2 are null matrices of size 4×2 and 4×5, respectively.

References

ANSYS, 1997. ANSYS 5.6 User's Manual. Swanson Analysis Systems Inc.

Bhaskar, K., Vardan, T.K., 1991. A higher-order theory for bending analysis of laminated shells of revolution. Computers and Structures 40, 815–819.

Bhaskar, K., Varadan, T.K., Ali, J.S.M., 1996. Thermoelastic solutions for orthotropic and anisotropic composite laminates. Composites: Part B 27, 415–420.

Bhimaraddi, A., 1984. A higher-order theory for free vibration analysis of circular cylindrical shells. International Journal of Solids and Structures 20, 623–630.

Cheung, Y.K., Cao, Z., Yuan, Z., Jian, X., 1991. Transient response of cylindrical shells with arbitrary shaped sections. Thin-walled structures 11, 305–318.

Di Sciuva, M., Icardi, U., 1993. Discrete-layer models for multilayered anisotropic shells accounting for the interlayers continuity conditions. Meccanica 28, 281–291.

Ganapathi, M., Makhecha, D.P., 2001. Free vibration analysis of multi-layered composite laminates based on an accurate higher-order theory. Composites, Part B; Engineering 32, 535–543.

Ganapathi, M., Patel, B.P., Pawargi, D.S., Patel, H.G., 2002. Comparative dynamic studies of thick laminated composite shells based on higher-order theories. Structural Engineering and Mechanics 13, 695–711.

He, L.H., 1994. A linear theory of laminated shells accounting for continuity of displacement and transverse shear stresses at layer interfaces. International Journal of Solids and Structures 31, 613–627.

Herakovich, C.T., 1998. Mechanics of Fibrous Composites. John Wiley, New York.

Hui, D., Du, H.Y., 1986. Effects of axial imperfections on vibrations of anti-symmetric cross-ply, oval cylindrical shells. Journal of Applied Mechanics 53, 675–680.

Icardi, U., 1998. Cylindrical bending of laminated cylindrical shells using a modified zigzag theory. Structural Engineering and Mechanics 5, 497–516.

Kraus, H., 1967. Thin Elastic shells. John Wiley, New York.

Kumar, V., Singh, A.V., 1995. Vibrations of composite noncircular cylindrical shells. Journal of Vibration and Acoustics 117, 471–476.

Kumar, V., Singh, A.V., 1996. Vibrations of fibre-reinforced deep shells. Journal of Pressure Vessel Technology 118, 407–414.

Leech, J.N., 1965. Stability of finite difference equations for the transient response of a flat plate. American Institute of Aeronautics and Astronautics Journal 3, 1772–1773.

Leissa, A.W., 1973. Vibration of shells. NASA SP-288.

Makhecha, D.P., Ganapathi, M., Patel, B.P., 2001a. Dynamic analysis of laminated composite plates subjected to thermal/mechanical loads using an accurate theory. Composite Structures 51, 221–236.

Makhecha, D.P., Ganapathi, M., Patel, B.P., 2001b. A shear flexible shell element based on higher-order realistic theory for dynamic analysis. In: Proceedings of International Conference on Theoretical, Applied, Computational and Experimental Mechanics, 27–30 December, Kharagpur, India.

Makhecha, D.P., Patel, B.P., Ganapathi, M., 2001c. Transient dynamics of thick skew sandwiches laminates under thermal/mechanical loads. Journal of Reinforced Plastics and Composites 20, 1524–1545.

Murukami, H., 1986. Laminated composite plate theory with improved in-plane responses. ASME Journal of Applied Mechanics 53, 661–666.

Noor, A.K., 1973. Noncircular cylinder vibration by multilocal method. In: Proc ASCE 99, Engineering Mechanics Division, pp. 389–407.

Noor, A.K., 1990. Bibliography of monographs and surveys on shells. Applied Mechanics Review 43, 223–234.

Noor, A.K., Burton, W.S., 1990. Assessment of computational models for multilayered composite shells. Applied Mechanics Review 43, 67–97.

Pratap, G., 1985. A C^0 continuos 4-noded cylindrical shell element. Computers and Structures 21, 995–999.

Qatu, M.S., 1992. Review of shallow shell vibration research. Shock Vibration Digest 24, 3–15.

Qatu, M.S., 1999. Accurate equations for laminated composite deep thick shells. International Journal of Solids and Structures 36, 2917–2941.

Rao, S.R., Ganesan, N., 1996. Interlaminar stresses in shells of revolution. Mechanics of Composite Materials and Structures 3, 321–339.

Soldatos, K.P., 1984. A Flugge-type theory for the analysis of anisotropic laminated non-circular cylindrical shells. International Journal of Solids and Structures 20, 107–120.

Soldatos, K.P., 1987. Free vibration analysis of thickness shear deformable cross-ply laminated oval shells. In: Elishakoff, I. et al. (Eds.), Refined Dynamical Theories of Beams, Plates and Shells Lecture Notes in Engineering, vol. 28. Springer, Berlin, pp. 324–332.

Soldatos, K.P., 1994. Review of three-dimensional dynamic analysis of circular cylinders and cylindrical shells. Applied Mechanics Review 47, 501–516.

Soldatos, K.P., 1999. Mechanics of cylindrical shells with non-circular cross-section: a survey. Applied Mechanics Review 52, 237–274.

Soldatos, K.P., Tzivanidis, G.J., 1982. Buckling and vibration of cross-ply laminated non-circular cylindrical shells. Journal of Sound and Vibration 82, 425–434.

Subbaraj, K., Dokainish, M.A., 1989. A survey of direct time-integration methods in computational structural dynamics II: Implicit methods. Computers and Structures 32, 1387–1401.

Suzuki, K., Shikanai, G., Leissa, A.W., 1994. Free vibrations of laminated composite thin non-circular cylindrical shell. Journal of Applied Mechanics 61, 861–871.

Suzuki, K., Shikanai, G., Leissa, A.W., 1996. Free vibrations of laminated composite thick noncircular cylindrical shell. International Journal of Solids and Structures 33, 4079–4100.

Tsui, T.Y., Tong, P., 1971. Stability of transient solution of moderately thick plates by finite difference methods. American Institute of Aeronautics and Astronautics Journal 9, 2062–2063.

Ye, J.Q., Soldatos, K.P., 1997. Three-dimensional vibrations of cross-ply laminated hollow cylinders with clamped edge boundaries. ASME Journal of Vibration and Acoustics 119, 317–323.

Zienkiewicz, O.C., 1971. Finite Element Methods in Engineering Science. McGraw-Hill, London.